

PHENIX results of π^0 -hadron correlations

Cheuk-Ping Wong* †

Georgia State University

E-mail: cwong14@student.gsu.edu

High momentum partons lose energy in the QGP that is produced in heavy-ion collisions at RHIC, indicated by the fact that jets from these partons are broadened and less energetic when compared to jets in $p + p$ collisions. This in turn indicates that measurements of jet broadening and energy loss provide important insights to the transport properties of the QGP. In PHENIX, information about the jet width and energy loss is extracted from two-particle angular correlation functions of neutral pions and charged hadrons in Au+Au collisions. Background flow is subtracted from the correlation functions of Au+Au data with measured flow harmonic coefficients (v_n) from PHENIX. Acoustic Scaling is used to estimate the higher order ($n = 3, 4$) v_n values, which have not been measured at high p_T at RHIC. The comparison of Au+Au to $p + p$ results shows jet broadening and away side enhancement in the low associated p_T region. Details of the Au+Au analysis, the latest results in small systems, and physics implications are discussed.

*13th International Workshop on High- p_T Physics in the RHIC/LHC era
March 19th 2019
Knoxville, Tennessee*

*Speaker.

†For the PHENIX Collaboration

1. Introduction

Since hard scattered partons lose energy as they traverse the Quark-Gluon Plasma (QGP) created in heavy-ion collisions, such as Au+Au, the fragmented jets from these partons are modified, meaning they are broader and less energetic. Thus, jet modification relative to $p + p$ jet measurements study can be used to probe the properties of the QGP [1].

2. π^0 -Hadron Correlation Analysis

The soft background dominates over jet signal at RHIC energies. In addition, the limited azimuth and rapidity acceptances of PHENIX make full jet reconstruction even more challenging. Therefore, instead of using full jet reconstruction, two-particle azimuth ($\Delta\phi$) correlations are measured in PHENIX to probe jets. In PHENIX, the common two-particle correlations species are direct gamma-hadron, and hadron-hadron. Although direct gamma-hadron correlations give access to parent parton initial transverse momentum, direct photons are overwhelmed by large decay photon background from π^0 decays at RHIC. In the case that statistics is crucial, such as Au+Au measurement which suffers from subtraction of strong underlying events, π^0 -hadron correlation analysis is complementary.

The electromagnetic calorimeters (EMCal) with fine spatial resolution in PHENIX central arm is used to measure decay photon pairs. These decay photon pairs are reconstructed to neutral pions in 4–15 GeV/c. Reconstructed neutral pions within 0.12–0.16 GeV mass window are selected as trigger particles. The drift and pad chamber detectors are also used for charged hadron tracking in 0.5–7 GeV/c with the help of RICH detector to veto electron tracks below 5 GeV/c.

Azimuthal correlation functions are corrected with detector efficiency obtained from PHENIX GEANT3 simulation. Event-mixing is performed to correct $\Delta\phi$ for effects due to PHENIX's central arms geometry. The contribution from combinatorial background π^0 is accounted for in the systematic uncertainty and is estimated using the side-band π^0 in the 0.08 – 0.11 GeV and 0.165 – 0.2 GeV mass windows. The underlying event is assumed to have a flat distribution in $p + p$ data. In Au+Au data, however, one needs to account for the contribution of flow raised by initial collision geometry. The spatial correlation of the underlying event due to flow can be described as a Fourier series in $\Delta\phi$ as shown in Eq. (2.1)

$$\frac{dN_{flow}}{d\Delta\phi}(\Delta\phi) = b_0 \left[1 + \sum v_n^{\pi^0} v_n^h \cos(n \cdot \Delta\phi) \right] \quad (2.1)$$

where b_0 is the level of the underlying event obtained from the Absolute Normalization Method [2]. As demonstrated in several experimental observables [3, 4, 5], the coefficients of flow harmonics in the interested p_T regions can be factorized to $v_n^{\pi^0}$ and v_n^h which are the n th order flow harmonic coefficients for π^0 and charged hadron, respectively. While v_n^h ($n = 2, 3, 4$) and $v_2^{\pi^0}$ are interpolated from PHENIX results [6, 7], higher order $v_n^{\pi^0}$ have not been measured at RHIC in the high momentum region. To estimate $v_3^{\pi^0}$ and $v_4^{\pi^0}$, Acoustic Scaling [8] is applied. Acoustic Scaling refers to the ratio of v_n ($n = 3, 4$) to $(v_2)^{n/2}$, that is,

$$g_n = \frac{v_n}{(v_2)^{n/2}}. \quad (2.2)$$

This ratio, denoted as g_n , is p_T independent up to 10 GeV/c as demonstrated with PHENIX data [8]. Thus, we can obtain charged hadron g_n^h with existing PHENIX charged hadron v_n^h results

$$g_n^h = \frac{v_n^h}{(v_2^h)^{n/2}}, \quad (2.3)$$

and assuming $g_n^h = g_n^{\pi^0}$ then apply Eq. (2.2) again to estimate neutral pion $v_3^{\pi^0}$ and $v_4^{\pi^0}$ via

$$v_n^{\pi^0} = g_n^h (v_2^{\pi^0})^{n/2}. \quad (2.4)$$

3. Angular Broadening in Au+Au Results

Results from 2007 PHENIX Au+Au data [5] only removed second order flow harmonics with the assumption that the higher even order flow harmonics are negligible, and the odd order flow harmonics do not exist in heavy-ion collisions. In fact, the third order flow harmonics, which is due to the fluctuations in the initial collision geometry, is non-zero as demonstrated with PHENIX and STAR, and PHOBOS data [7, 9, 10]. This third order triangular flow contributes to the shoulder shape of the away-side of the jet functions. In order to eliminate flow effects and extract jet functions, higher flow harmonics up to the fourth order are subtracted in the present analysis which is using combined 2010 and 2011 PHENIX 200 GeV Au+Au data.

Examples of jet functions from combined 2010 and 2011 PHENIX 200 GeV Au+Au data in 0–20% and 20–40% centrality are shown in Fig. 1 and 2 with Gaussian fits. These new results have subtracted second, third, and fourth order underlying flow harmonics. The away-side jet shape is closer to a Gaussian shape compared to the previous PHENIX results [5] which subtracted the second order flow harmonics only. This improvement is more obvious in the low p_T bins where underlying flow is strongest.

The away-side jet width is extracted from the Gaussian fits as shown in Fig. 3 which shows the away-side width decreases as trigger or associate p_T increases. Furthermore, the away-side width in the most central events is reduced compared to the old results [5] as the away-side jet functions become more Gaussian with higher order flow harmonics subtracted. However, jet broadening in Au+Au results is still observed in the low p_T regions compared to $p+p$ results. As the associate p_T increases, the Au+Au and $p+p$ results converge. Comparing 0–20% and 20–40% Au+Au results, the centrality dependence is insignificant as the uncertainties of these two centrality ranges overlap.

4. p_{out} Broadening in Small Systems

Besides the spatial correlations in the azimuth $\Delta\phi$, one can also study two-particle correlations in momentum space by studying p_{out} distributions. p_{out} written in Eq. (4.1) is defined as the transverse component of associated particle p_T^{assoc} with respect to the trigger particle p_T^{trig} [11, 12]. In Eq. (4.1), $\Delta\phi$ is the azimuth angle between the trigger and associated particles as described in Section 2.

$$p_{out} = p_T^{assoc} \cdot \sin(\Delta\phi) \quad (4.1)$$

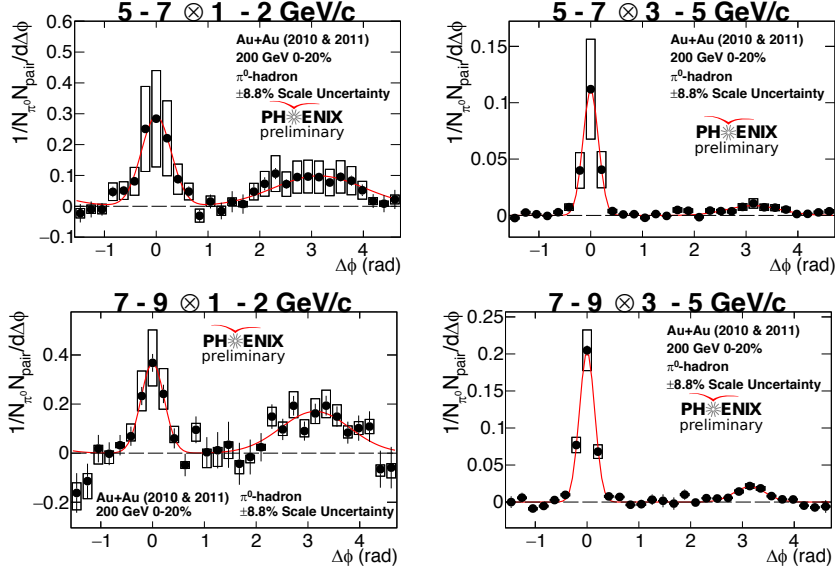


Figure 1: Jet functions with Gaussian fits (red lines) in 0–20% centrality.

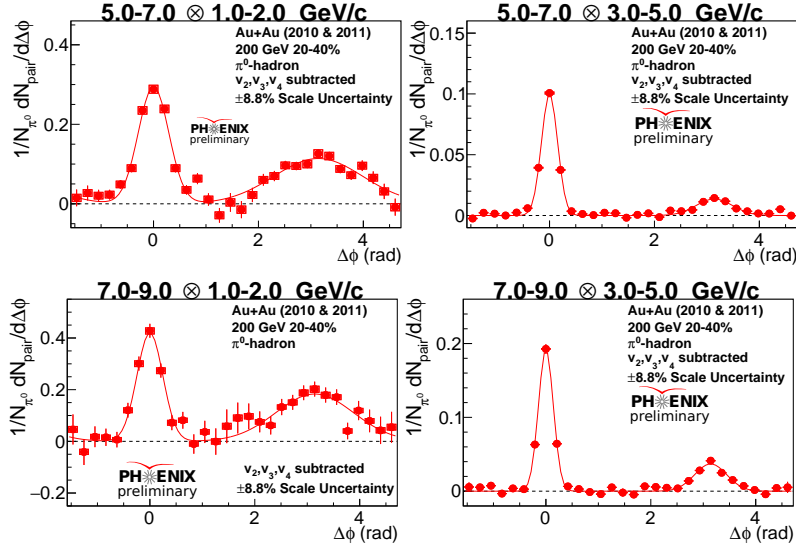


Figure 2: Jet functions with Gaussian fits (red lines) in 20–40% centrality.

The near-side and away-side p_{out} distributions from PHENIX 2015 $p+p$ and $p+Au$ data are shown in Fig. 4. The color scheme in Fig. 4 separates p_{out} distributions in different x_E ranges. x_E , defined in Eq. (4.2), is the longitudinal fraction of the p_T^{assoc} to the p_T^{trig} . The x_E can serve as an approximation of z which is the ratio of the longitudinal momentum of the away-side jet to the near-side jet in full jet reconstruction [11].

$$x_E = -\frac{|p_T^{assoc}|}{|p_T^{trig}|} \cos(\Delta\phi) \quad (4.2)$$

Demonstrated in Fig. 4, the away-side p_{out} distributions are broader than the near-side. This is due to the fact that away-side p_{out} depends on the initial parton momentum while the near-side p_{out} does not [12]. Hence, the away-side p_{out} variation is wider than the near-side p_{out} .

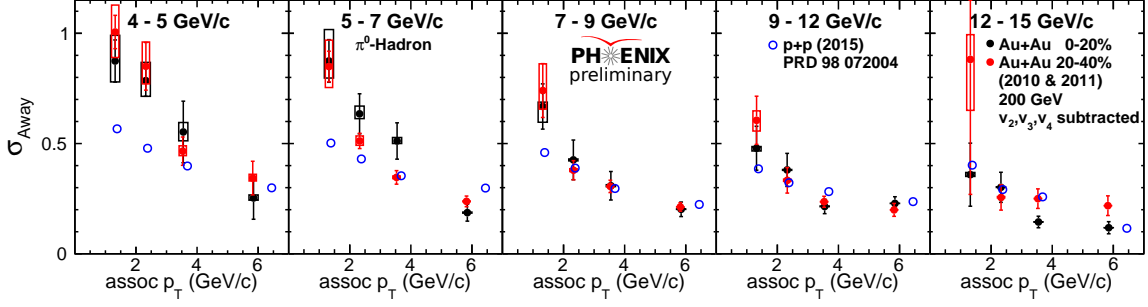


Figure 3: Away-side jet Gaussian width. Results from 200 GeV Au+Au in 0–20% and 20–40% centralities are shown in black and red dots. Blue circles are PHENIX 2015 200 GeV $p + p$ results.

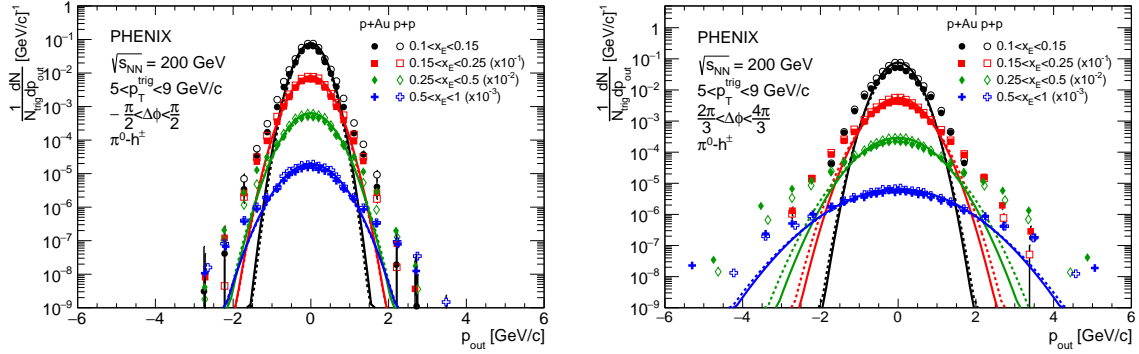


Figure 4: Near-side (left) and away-side (right) p_{out} distributions in different x_E ranges from 200 GeV $p + p$ (solid dots) and $p+Au$ (open circles) data. The solid and dash lines are the Gaussian fits in the nonperturbative region [12].

The difference of the squared Gaussian width $\langle p_{out}^2 \rangle$ extracted from p_{out} distributions from 200 GeV $p + p$, $p+Al$, and $p+Au$ data is plotted as a function of x_E as shown in Fig. 5. Figure 5 shows no near-side p_{out} broadening in both $p+Al$ and $p+Au$ systems compared to $p + p$ system. In the away side, however, p_{out} broadening in the $p+Au$ system is observed, and the broadening enhances in higher x_E .

Focus on $0.15 < x_E < 0.25$ and $0.25 < x_E < 0.5$, difference of away-side $\langle p_{out}^2 \rangle$ as a function of N_{coll} is shown in Fig. 6 which demonstrates that p_{out} is further broadened as N_{coll} increases. This N_{coll} dependence could be caused by initial transverse momentum enhancement during multiple hard scattering in the initial collision stage [13, 14].

5. Conclusion

This presentation gave details in 2010 and 2011 π^0 -hadron correlation analysis using data from Au+Au and small systems collisions measured at PHENIX. The updated Au+Au analysis removes the effect of flow harmonics up to the fourth order. The new jet functions in low p_T show a more Gaussian shape in the away-side peak than the previous PHENIX results which did not subtract third order flow harmonics. However, the away-side jet broadening still remains in the low associated p_T region compared to $p + p$ results. As the associated p_T rises, the away-side widths from Au+Au and $p + p$ results converge. There is no centrality dependence observed in away-side

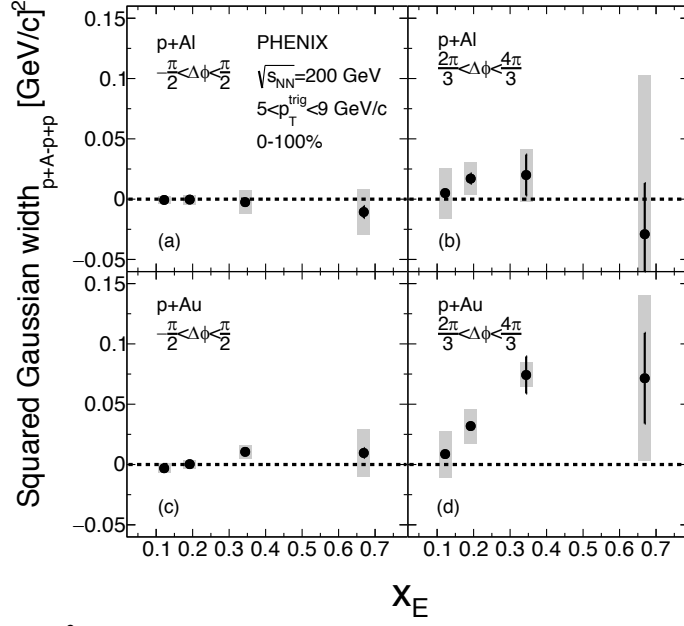


Figure 5: Difference in $\langle p_{out}^2 \rangle$ as a function of x_E . Top row is 200 GeV p +Al results in full centrality range, bottom row is 200 GeV p +Au results in full centrality range. Left and right columns are difference in $\langle p_{out}^2 \rangle$ from near and away side measurements, respectively [12].

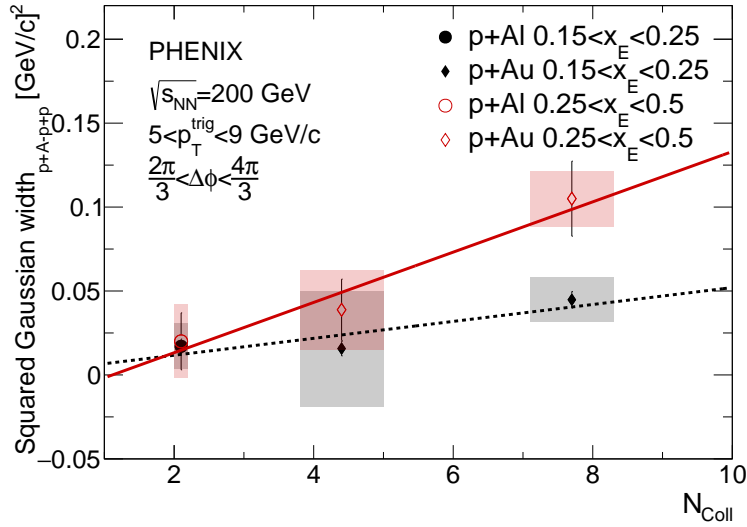


Figure 6: Difference in $\langle p_{out}^2 \rangle$ as a function of N_{coll} . Results in 0.15–0.25 and 0.25–0.5 x_E bins are drawn in black and red, respectively. p +Al results are drawn in circle or dot markers, while open and solid diamond markers represent p +Au results. The red and black lines are linear fits to the data [12].

widths from the comparison of 0–20% to 20–40% centrality ranges as the uncertainties in these ranges overlap.

Jet broadening in small systems is also shown in momentum space in the study of p_{out} . While modification of the near-side p_{out} is not observed, away-side p_{out} broadening is shown in p +Au data compared to $p + p$. Indication of correlation between away-side p_{out} broadening and N_{coll} is found. These observations could be due to boost of initial transverse momentum in the beginning

of collision. These results, which give insight to cold nuclear matter effects, are also important for understanding hot nuclear matter effect in the study of QGP medium in heavier systems.

Acknowledgments

This work was supported by the National Science Foundation [grant number 1714802].

References

- [1] M. Connors, C. Nattrass, R. Reed, S. Salur, Jet measurements in heavy ion physics, *Rev. Mod. Phys.* 90 (2018) 025005. doi:10.1103/RevModPhys.90.025005.
- [2] A. Sickles, M. P. McCumber, A. Adare, Extraction of correlated jet pair signals in relativistic heavy ion collisions, *Phys. Rev. C* 81 (2010) 014908. doi:10.1103/PhysRevC.81.014908.
- [3] J. Adam, et al., Jet-like correlations with neutral pion triggers in pp and central pb-pb collisions at 2.76 TeV, *Physics Letters B* 763 (2016) 238 – 250. doi:10.1016/j.physletb.2016.10.048.
- [4] L. Adamczyk, et al., Jet-like correlations with direct-photon and neutral-pion triggers at $\sqrt{s_{NN}} = 200$ GeV, *Physics Letters B* 760 (2016) 689 – 696. doi:10.1016/j.physletb.2016.07.046.
- [5] A. Adare, et al., Transition in yield and azimuthal shape modification in dihadron correlations in relativistic heavy ion collisions, *Phys. Rev. Lett.* 104 (2010) 252301. doi:10.1103/PhysRevLett.104.252301.
- [6] A. Adare, et al., Measurement of two-particle correlations with respect to second and third-order event planes in Au+Au collisions at $\sqrt{s_{NN}} = 200$ GeV, *Phys. Rev. C* 99 (2019) 054903. doi:10.1103/PhysRevC.99.054903.
- [7] A. Adare, et al., Measurements of higher-order flow harmonics in au+au collisions at $\sqrt{s_{NN}} = 200$ GeV, *Phys. Rev. Lett.* 107 (2011) 252301. doi:10.1103/PhysRevLett.107.252301.
- [8] R. A. Lacey, et al., Scaling of the higher-order flow harmonics: implications for initial-eccentricity models and the.
- [9] L. Adamczyk, et al., Third harmonic flow of charged particles in au + au collisions at $\sqrt{s_{NN}} = 200$ gev, *Phys. Rev. C* 88 (2013) 014904. doi:10.1103/PhysRevC.88.014904.
- [10] B. Alver, G. Roland, Collision-geometry fluctuations and triangular flow in heavy-ion collisions, *Phys. Rev. C* 81 (2010) 054905. doi:10.1103/PhysRevC.81.054905.
- [11] C. Aidala, et al., Nonperturbative transverse-momentum-dependent effects in dihadron and direct photon-hadron angular correlations in $p + p$ collisions at $\sqrt{s} = 200$ GeV, *Phys. Rev. D* 98 (2018) 072004. doi:10.1103/PhysRevD.98.072004.
- [12] C. Aidala, et al., Nonperturbative-transverse-momentum broadening in dihadron angular correlations in $\sqrt{s_{NN}} = 200$ GeV proton-nucleus collisions, *Phys. Rev. C* 99 (2019) 044912. doi:10.1103/PhysRevC.99.044912.
- [13] J. W. Cronin, et al., Production of hadrons at large transverse momentum at 200, 300, and 400 gev, *Phys. Rev. D* 11 (1975) 3105–3123. doi:10.1103/PhysRevD.11.3105.
- [14] M. Corcoran, et al., Evidence for multiple scattering of high energy partons in nuclei, *Physics Letters B* 259 (1) (1991) 209 – 215. doi:https://doi.org/10.1016/0370-2693(91)90160-R.